



# Comparison of Turbine Discharge Measured by Current Meters and Acoustic Scintillation Flow Meter at Laforge-2 Power Plant

David D. Lemon, ASL Environmental Sciences Inc., Sidney, B.C.  
Nicolas Caron, Hydro-Québec, Montréal, Québec  
Ward W. Cartier, ASL Environmental Sciences Inc., Sidney, B.C.  
Gilles Proulx, Hydro-Québec, Montréal, Québec

---

## Abstract

Performance tests were conducted at Unit 22 at Hydro-Québec's Laforge-2 plant between June 11 and 15, 1997. These tests included measurements of the discharge through the turbine using current meters. Simultaneous measurements were also taken in one bay of the intake with an Acoustic Scintillation Flow Meter (ASFM). The ASFM is a new instrument which offers unique advantages for measuring intake flows in low-head, short intake plants for which current meters have been the traditional and only effective method. It is non-intrusive, and its deployment in intake gate slots is straightforward, allowing data to be collected with a minimum of plant downtime. Laforge-2 is typical of large to medium-sized plants of that type: it is equipped with two 147 MW Kaplan turbines, each with a three-bay intake. The bays at the metering section are 19.7m high and 6.1m wide. The net head for the plant is 27.4m.

The current metering used one hundred ninety measuring points in each bay, obtained using forty individual current meters mounted in four rows of 10 on a frame 4.6m high. The current meter rows were spaced 1.08m apart vertically. The inclination of the meters was controlled by a hydraulic adjustment system to align them with the flow. The ASFM transducer arrays were mounted on the same frame as the current meters in Bay 1, at the trailing (downstream) edge of the frame. Flow measurements were taken simultaneously with the current meters and the ASFM at a series of unit operating conditions. Measurements were taken using two different profiling methods: one with the frame at five fixed positions, using data from all four rows, the other with the frame profiling continuously, using data from the lowest row on the frame.

The trash racks had been removed from the intakes for the testing, resulting in low levels of turbulence in the flow. The low turbulence, combined with interference from the current meters mounted ahead of the ASFM transducers, hampered the performance of the ASFM when the fixed-position measurements were taken. The interference was least at the lowest array pair, which allowed meaningful data to be obtained during most of the profiling runs. The discharge through the bay was independently computed for twelve cases (between 145 and 200 m<sup>3</sup>/sec), and the results then compared. Over this range the mean difference between the measurements was 1.6%. An analysis of the differences and the uncertainties in both methods is made. The results of the analysis are used to assess the ASFM's advantages for measuring turbine flows in low-head plants.

## Introduction

The turbine testing programme at Laforge-2 presented an opportunity to compare the performance of the ASFM with that of current meters in measuring discharge at a low-head plant. The planned current meter measurements were to use mounting frames that were capable of being adapted to mount the transducers for the ASFM. Simultaneous measurements could then be made with both methods, thus allowing a direct comparison of their results. Hydro-Québec agreed to provide access and logistical support at the site and to make available comparison data from current meter measurements. ASL Environmental Sciences provided the ASFM and the labour required to install and operate it. The test and measurement programme for the turbine was not altered; the ASFM measurements were to be made as circumstances permitted in the course of the planned operations.

The ASFM is a non-intrusive acoustic method for measuring flow, which has some unique advantages for discharge measurement in low-head plants. It uses acoustic scintillation drift, a technique for measuring flows in a turbulent medium, such as water or air, by analyzing the variations (with position and time) of sound which has passed through it. Scintillation in this context refers to random variations in the intensity of the sound caused by the variations in the refractive index of the water produced by the turbulence which is always present in any natural flow. The ASFM measures the speed of the current from the transverse drift of the acoustic scintillations observed across two relatively closely-spaced propagation paths. The method has been used for many years to measure winds in the atmosphere and ionosphere (Ishimaru, 1978; Lawrence, Ochs & Clifford, 1972; Wang, Ochs & Lawrence, 1981), for measuring currents and turbulence in ocean channels (Clifford & Farmer, 1983; Farmer & Clifford, 1986; Farmer, Clifford & Verrall, 1987; Lemon & Farmer, 1990; Lemon, 1993) and in hydroelectric plants (Birch & Lemon, 1993; Lemon, 1995; Lemon & Bell, 1996); its derivation is well-established.

Figure 1 shows a schematic representation of an ASFM in use. Two transmitters are placed at one side of the channel, two receivers at the other. The signal amplitude at the receivers varies randomly in time as the distribution of turbulence along the propagation paths changes with time and the flow of the mean current. If the paths are sufficiently closely-spaced, the turbulence may be regarded as being embedded in the mean flow, and then the pattern of scintillations at the downstream receiver will be nearly identical to that at the upstream receiver, except for a time delay,  $Dt$ . The delay is found by computing the time-lagged cross-correlation between the signal amplitudes at the two receivers over some suitable length of record.  $Dt$  is then the lag at which the peak of the cross-correlation function is found, and the mean flow speed perpendicular to the acoustic beams is  $Dx/Dt$ , where  $Dx$  is the separation between the beams.

The ASFM measures the lateral (i.e. along-path) average of the component of the flow perpendicular to the acoustic path. It is therefore well-suited to collecting data for discharge measurements, since the product of the path length with the lateral average of the normal component of flow gives the element of discharge at the depth of the path. Sampling at several levels in the vertical and integrating then gives the discharge.

The ASFMs inherent suitability for discharge measurements, combined with its non-intrusive nature results in a number of advantages for measuring the discharge through turbines. The discharge measurement can be made in an intake gate slot, as it requires only that the transducers be installed at several levels along the sides. This can be a great advantage for low-head plants, where intake tunnels are often short, and do not have any straight segments with constant cross-section. The spatial averaging which is part of the ASFMs measurement means also that large-scale eddies and meandering do not bias the measurement.

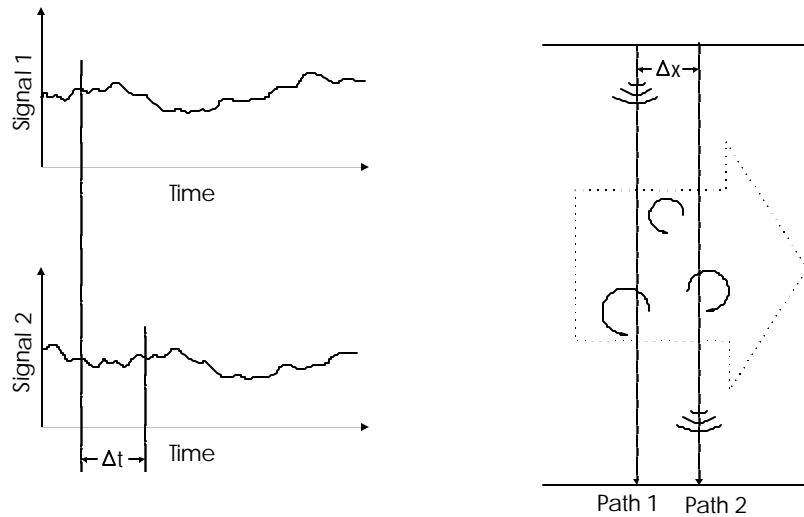


**Figure 1: Schematic representation of current measurement by acoustic scintillation.**

Measurement of the discharge for a turbine requires that a location in the intake be chosen to establish the measurement plane, and a number of sampling paths be established across it. The transducer arrays can either be fixed to the intake walls, for a permanent installation, or attached to a frame deployed into a gate slot, if one is available. Using a frame in a gate slot allows the ASFMs to be moved from one unit to another relatively quickly and easily, if the slots are all the same size. The number of paths required to sample in the vertical is achieved either by placing arrays at every desired height on the frame, or by using fewer arrays and moving the frame to the required elevations. In either case, the discharge is computed by integrating the horizontal component of the laterally-averaged velocity over the height of the intake.

## Measurements

### Current Meter Installation

The flow measurements by current meter were performed using a set of 120 current meters mounted on three frames (Figure 2). Each frame consisted of two carriages which slid into the gate slots. The carriages were joined by four ovoid rods (Figure 3) to which the current meters were attached by means of an oblique support. There were 10 current meters on each rod, giving a total of 40 per frame and 120 overall. The rods were spaced 1.08 metres apart in the vertical.

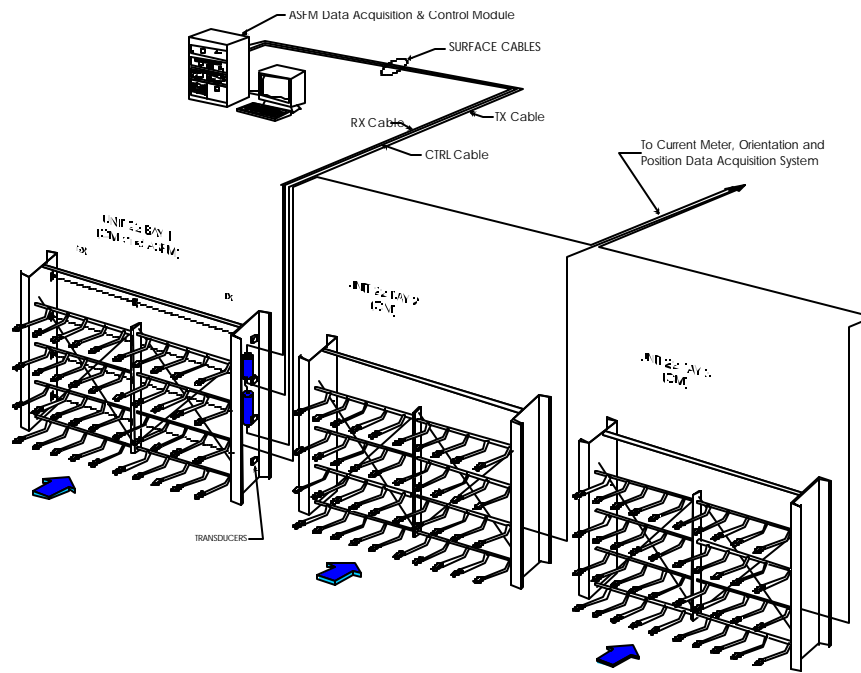


**Figure 2: ASF and CM system installations in bays 1, 2 and 3 of Unit 22.**

As the frames did not span the entire section, they were moved by means of electric hoists installed at the top of the gate slots. Details of the current meter mounting system may be found in Proulx & Lévesque (1996).

### ASF Mounting and Installation

The ASFM available for use at Laforge-2 could not be configured to measure in all three bays. Since the purpose of the measurements was to compare the discharge measured by the ASFM

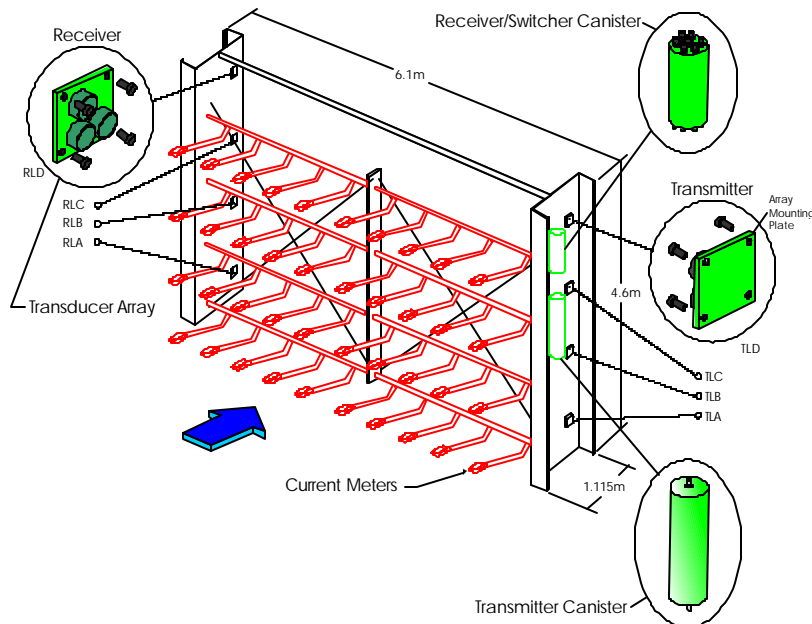


**Figure 3: Detailed ASF frame components.**

and the current meters, ASFM data were required from one bay only. Figure 2 shows the ASFM installed in Bay 1 of Unit 22, with the current meter arrays in all three bays. The frames carrying the current meters and the ASFM were installed in the outer most gate slot of all three intake bays (see Figure 6 below). ASFM surface cables consisting of RX, TX and CTRL cables were run from the frame up the gate slot and into the shutoff gate winch gallery where the data acquisition system was co-located with the CM data acquisition system. Facing downstream, the transmitter transducer arrays, receiver/switcher and transmitter canisters were mounted on the right side of the supporting frame and the receiver arrays were mounted on the left side, as shown in Figure 3. Four levels were mounted on the frame with level A being the bottom most level and level D being the upper most. Array element orientation was such that, for each level, opposing TX/RX pairs formed 3 separate acoustic paths. From these three paths both the horizontal and vertical components of the velocity could be resolved.

The transducer arrays were mounted on the frame into recessed holes with the outermost face of the transducers being flush with the face of the mounting frames. This allowed the faces of the array elements to be flush with the sides of the gate slot itself, providing an acoustic path length as close as possible to the actual width of the gate slot. Height measurements were taken from the base of the frame to a reference edge, on the array mounting plate, for all of the receiver and transmitter arrays on each side of the mounting frame. The height of a particular acoustic level, above the bottom of the frame, was then calculated from the average of the two measurements.

Work began mounting the ASFM hydrophones, canisters and cabling on June 9<sup>th</sup> and was completed that same day. The completed frame was installed in the gate slot on June 10<sup>th</sup> and preliminary tests were performed on the system.

### **Current Meter Data Collection**

Two procedures were used to sample the intake flow with the current meters. The first placed the frames at five different elevations at which data were collected from all the current meters. That produced 570 point measurements over the three bays for each flow condition. The second method, which was preferred because of the shorter execution time, swept the frames from the bottom of the intake to the top (or the reverse) and used only the lowermost row of 10 current meters on each frame. This method had the advantage that it sampled all of the section vertically. An important point in measuring the flow in a short convergent section like the one at Laforge-2 is the flow angle. The current meters used were not self-compensating, and therefore could not be placed horizontally to measure the horizontal component of the flow. The frames were equipped with a mechanism to rotate the mounting rods and align the current meters with the flow (Proulx & Lévesque, 1996).

The same mechanism serves to determine the flow angle. Previous experience at La Grande-1 (Proulx & Lévesque, 1996) has shown that the flow angle is quite different from a theoretical linear variation from the bottom (12.4 degrees) to the top (34.8 degrees). By altering the current meter angles with the mechanism and recording both the angle and velocity we can find the flow angle at the maximum velocity. As the flow is naturally disturbed due to the proximity of the intake, there is variability in the results. A least squares method is used to find a curve describing the flow angle as a function of elevation (Proulx & Caron, 1998).

## ASFM Data Collection

ASFM/CM comparison data in the profiling mode were taken over two consecutive days starting on June 14<sup>th</sup>, 1997 and finishing on June 15<sup>th</sup>. Data were collected for three flow conditions, shown in Table 1 below. For each of the 3 conditions, the tests were conducted off-cam with the blade angle held constant and a profile completed for a given wicket gate setting. Several profiles were done for various wicket gate settings. See Table 2 below.

**Table 1: Test flow condition descriptions.**

<i>Flow Condition</i>	<i>Description</i>
1	Off cam, 94% full blade angle, varied wicket gate opening.
2	Off cam, 73% full blade angle, varied wicket gate opening.
3	Off Cam, 53% full blade angle, varied wicket gate opening.

This resulted in four profile runs for each flow condition. Measurements were conducted simultaneously with both the CM and ASFM systems in each case.

**Table 2: Details of ASFM profile comparison data.**

<i>Date</i>	<i>Time</i>	<i>Flow Condition</i>	<i>Profile Number</i>	<i>Profile Direction</i>	<i>% Of Full Wicket Gate Setting</i>
14-06-97	19:35 – 20:12	1	70	↑	90
“	20:13 – 21:05	1	71	↓	87
“	21:06 – 21:40	1	72	↑	84
“	21:41 – 22:09	1	73	↓	93
15-06-97	14:02 – 14:29	2	80	↑	88
“	14:30 – 14:58	2	81	↓	85
“	14:59 – 15:28	2	82	↓	82
“	16:00 – 16:28	2	83	↑	91
“	19:35 – 20:01	3	85	↑	84
“	20:02 – 20:32	3	86	↓	81
“	20:33 – 20:59	3	87	↑	78
“	21:00 – 21:27	3	88	↓	86

## Results

### *ASFM Flow Velocities*

The absence of the trash racks reduced the level of turbulence present in the intake flow significantly. The amplitude scintillations were approximately 50% of those normally observed under similar flow conditions with trash racks in place. The low turbulence levels did not of

themselves impede the operation of the ASFM, however there were other interfering signals present which, combined with the low levels of turbulence, did impede the operation of the ASFM. The interference manifested itself as strong, coherent fluctuations in both amplitude and phase, as shown in Figure 4. Such interference is normally caused by vibration in the mounting

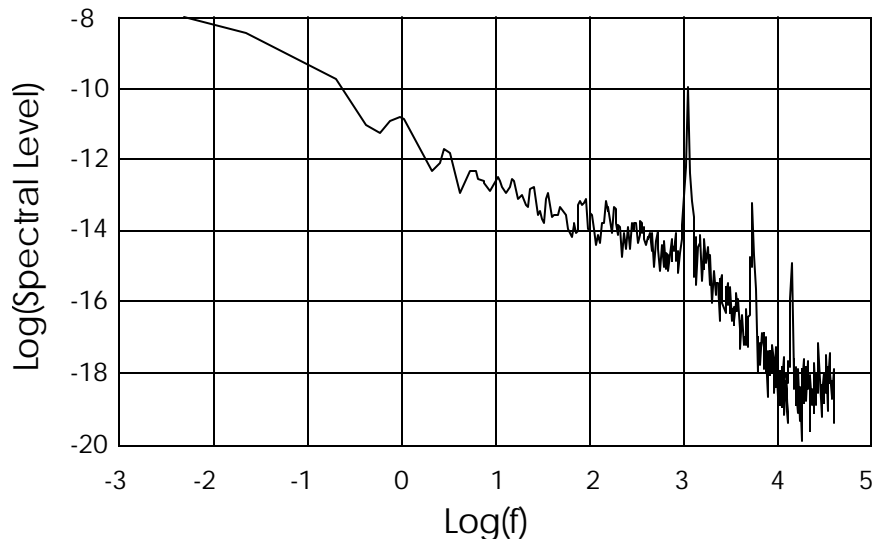


**Figure 4: Example of signal interference.**

frame, however in this case, the position sensors on the frames did not indicate significant vibration. It is more likely that, given the coherent nature of the interference, and its harmonic qualities as seen in Figure 4, it was an effect of the wakes of the current meters. The limitations imposed on the positioning of the ASFM transducers by the space available on the frame resulted in their being placed 90 cm downstream of the current meters, and exposed in varying degrees to the wake from the current meters, depending on the angle at which the meters were set. The ASFM's cross-correlation calculation depends on the scintillation time series being random, which is the case for natural turbulence. If the amplitude fluctuations are harmonic and coherent, then the cross-correlation function will have multiple peaks, whose position depends on both the current speed and the size of the structures producing the fluctuations. No unique solution for the flow speed then exists.

The harmonic nature of the interference suggested that removing it by filtering the amplitude data might be possible. Bandstop filters were individually designed for each path and each flow condition, since the composition of the interference changed with the position of the frame and the unit settings. Filtering proved consistently successful only for transducer set A (the lowest on the frame) at greater than minimum flow settings. In the other cases, the amount of interference was too great and the turbulence signal too low to obtain usable results in sufficient cases to compute discharges. Using path A in instances where the frame had been continuously swept over the intake did, however, allow discharges to be computed.

During a swept run, the ASFM collected data continuously over the period during which the frame was in motion. The ASFM data and the frame position data were recorded independently by the two groups, with alignment between the ASFM and positional data being provided by synchronisation of the clocks in the two systems.

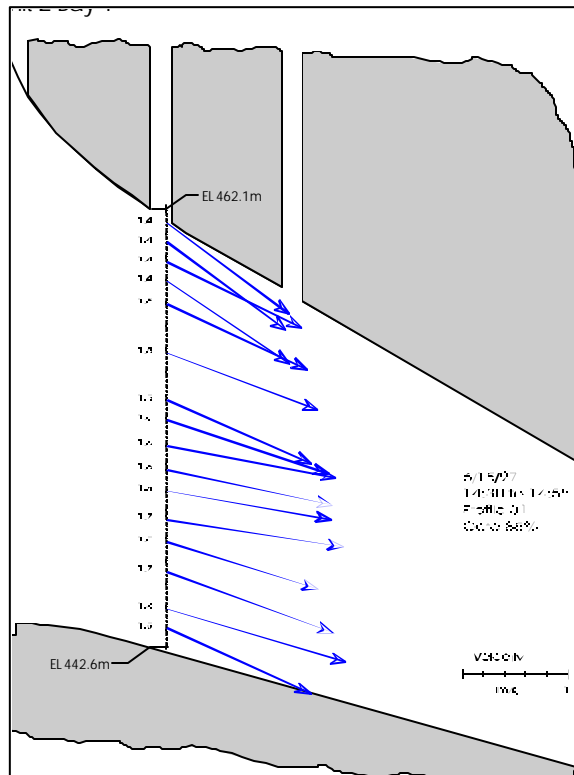
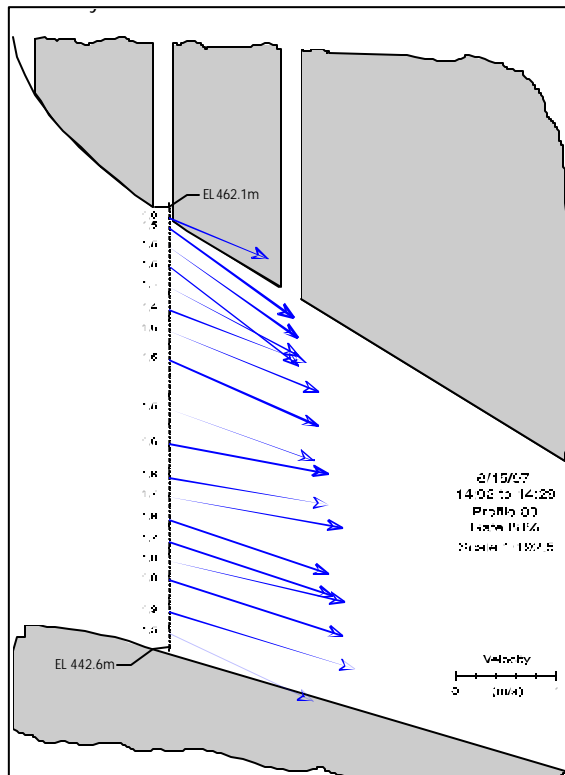
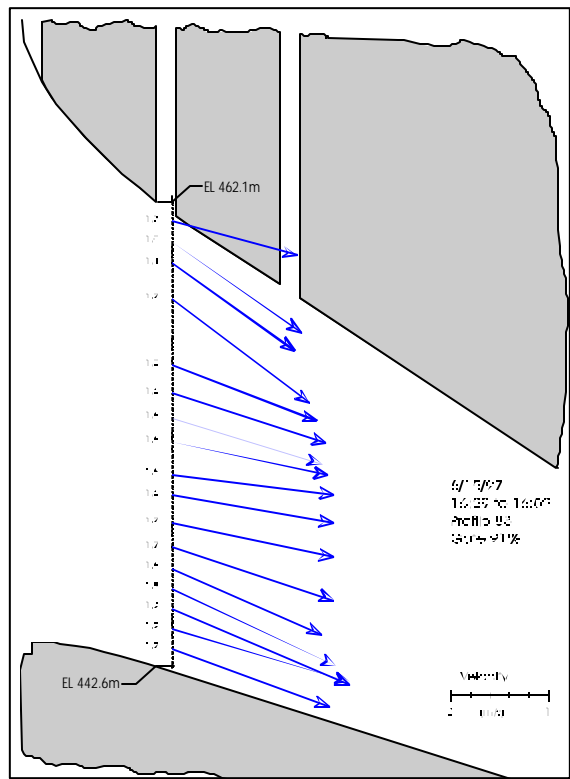
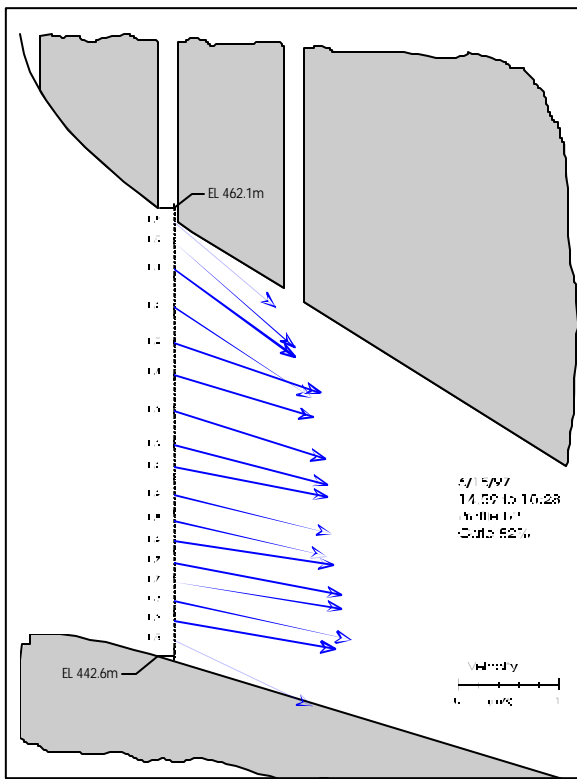


**Figure 5: Laterally-averaged ASFM velocity vectors.**



Each filtered ASFm data file was broken into 10.24-second blocks. The velocity was computed for each block and assigned an elevation corresponding to the midpoint of the block from the recorded elevation vs. time record. The velocity components were then averaged with elevation using a 4-sample running mean (approximately 0.5m elevation interval) and then sub-sampled at to the nearest 1 metre increments. The sub-sampled velocity components were then re-combined to form the laterally-averaged speed and inclination for each elevation point. Figure 5 shows an example of the results for four wicket gate settings with the turbine blades set at a fixed angle. The velocities are shown as scaled vectors on a cross-section of the intake. The number at the base of each arrow is the flow speed in m/sec.

### *ASFm Discharges*

Figure 6 shows the locations of the plane defined by the current meters and the plane defined by the ASFm transducers each time the frame traversed the intake. The ASFm plane was 0.9 metres downstream of the current meter plane. To facilitate the comparison between the two measurements, given this difference in location, the integrations for discharge were performed between 0.1022 and 19.422 metres elevation at the current meter section and 0.1 and 19.0 metres

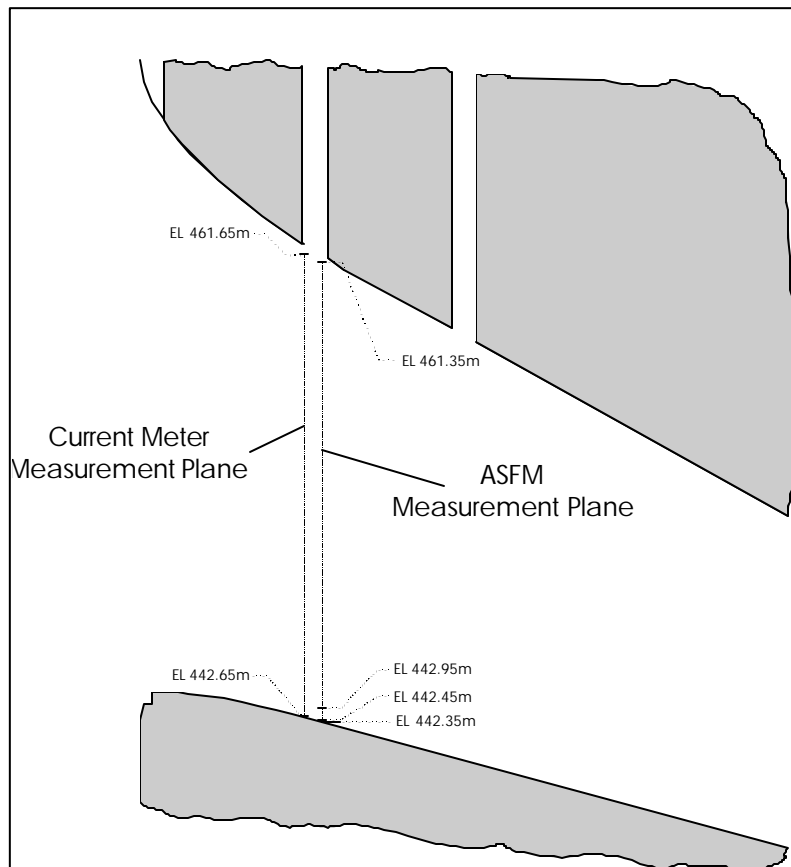


**Figure 6: Measurement planes and limits of integration.**

at the ASFM section. That was necessary because the height of the tunnel decreases by 0.42 metres between the current meter and ASFM planes, since the roof slope is steeper than the floor. The interval extended from the edge of the lower boundary layer to the point at which the effects of the upper boundary could be expected to appear. The discharge,  $Q$ , between those two limits is computed from the laterally-averaged velocity  $v$  as follows:

$$Q = \int_{0.1}^{19.0} v(z) \cos[q(z)] L dz \quad (1)$$

where  $v(z)$  is the magnitude of the laterally-averaged flow at elevation  $z$ ,  $q(z)$  is the corresponding inclination angle and  $L$  is the width between the transducer faces.

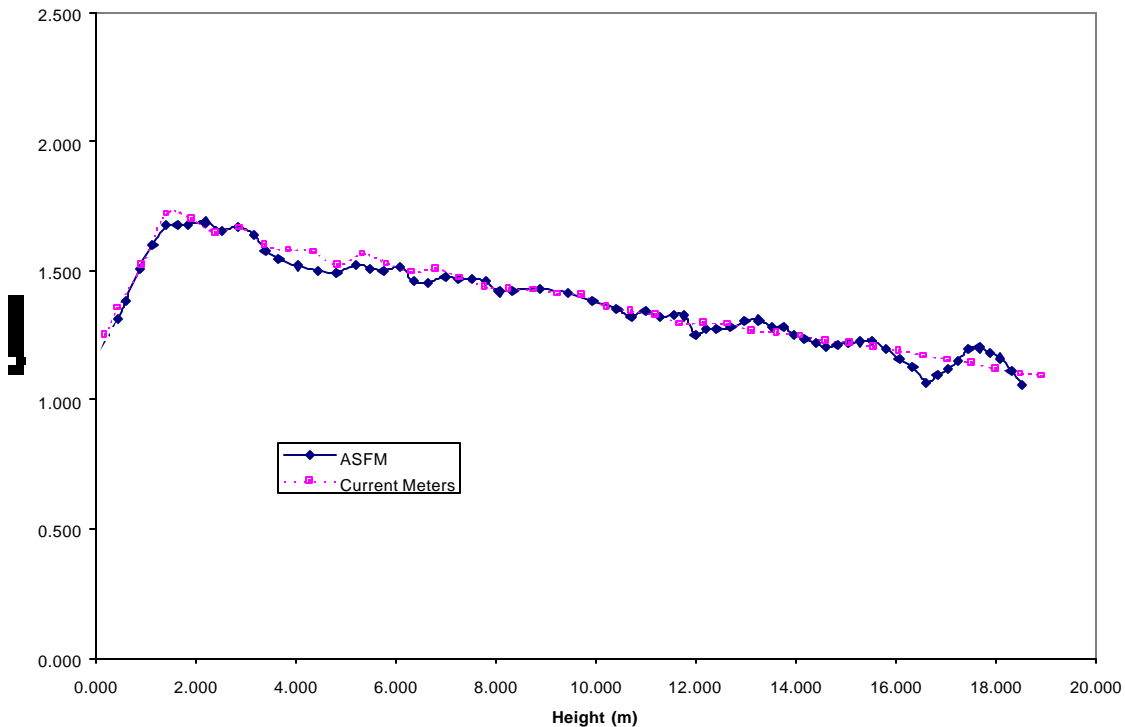


**Figure 7: Horizontal component of laterally-averaged velocity vs. height, profile #88, for ASFM and current meters. The current meter elevations have been scaled by a factor of 0.9782 and the current meter velocities by a factor of 1.0223 to account for the difference in the intake height at the two measurement locations.**

The integral was evaluated numerically, using a Romberg integration, with a cubic spline interpolation in the integrand between the measured points. Figure 7 shows an example of the horizontal component of velocity for both the ASFM and the current meters. The extrapolation of the ASFM data from the lowest measured point (0.6m) to the top of the boundary layer at the floor is shown as a dashed line, but is partially obscured by the current meter points. Discharges were computed for each of the 12 profile runs for which the filtering had produced usable results. Fifteen data sets had been collected; the three rejected were among the lower discharges. The discharges are listed in Table 3 below.

**Table 3: Comparison of discharges computed from current meters and ASFM.**

Run #	Q <sub>CM</sub> (m <sup>3</sup> /sec)	Q <sub>ASFM</sub> (m <sup>3</sup> /sec)	Diff. (%)	Run #	Q <sub>CM</sub> (m <sup>3</sup> /sec)	Q <sub>ASFM</sub> (m <sup>3</sup> /sec)	Diff. (%)
70	195.9	195.6	0.13	82	167.8	165.2	1.58
71	190.7	191.1	-0.24	83	180.8	176.6	2.36
72	185.6	181.7	2.15	85	157.3	152.9	2.90
73	200.7	197.5	1.64	86	153.4	149.4	2.69
80	178.0	172.9	2.94	87	148.3	149.5	-0.79
81	173.0	167.8	3.12	88	159.3	158.4	0.58

## Discussion

The discharges computed from the current meter data and from the ASFM for the same runs compared in Table 3 are shown graphically in Figure 8. The differences listed in the table are the ratio  $(Q_{CM}/Q_{ASFM})-1$ , expressed as a percentage. The average deviation between discharges

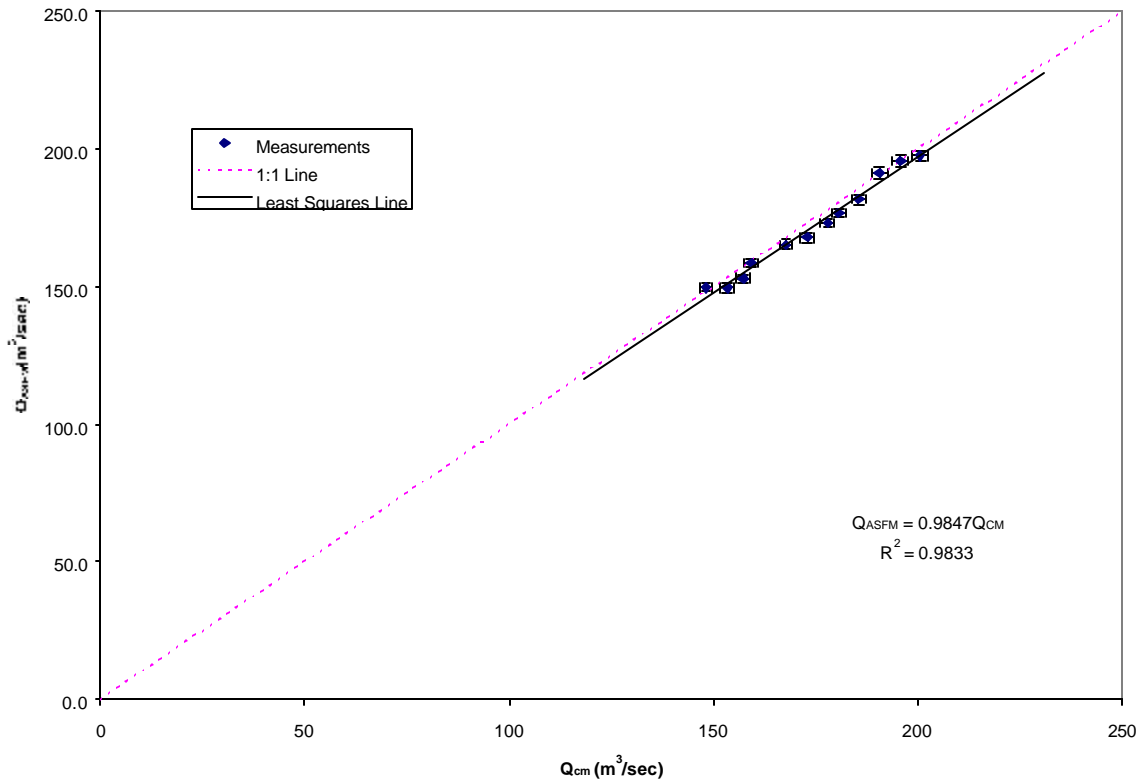


**Figure 8: Comparison of discharges measured by both methods**

in Table 3 is 1.8%; the maximum difference is 3.1%. The standard deviation of the differences about the mean is 1.3%. Figure 8 shows the two sets of discharges plotted against each other. The error bars on the points are  $\pm 1\%$ . The solid line is the least squares fit of the ASFM discharge against the current meter discharge. The slope of the line is 0.985, i.e. 1.5% less than exact agreement overall. The correlation coefficient is 0.98.

The mean difference between the ASFM discharges and those measured by the current meters indicates that there is a systematic difference in the results obtained by the two methods. The

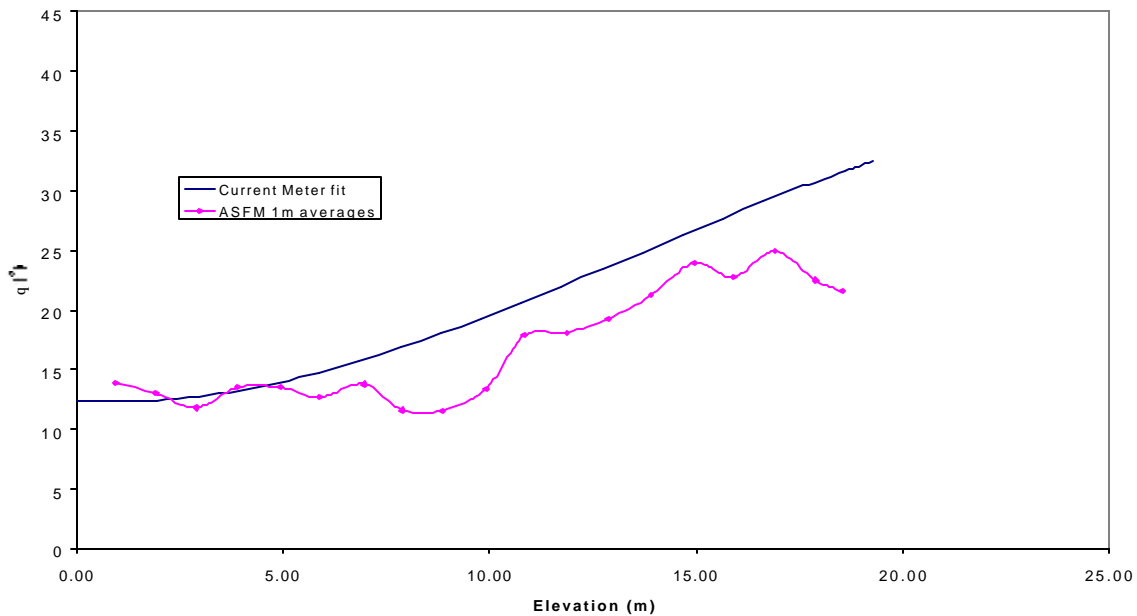


**Figure 9: Comparison of flow angle variation with height: curve fitted to current meter data and ASFM 1-metre averages. (Current meter curve scaled for difference in locations.)**

difference may arise either from the methods themselves, or from the difference in the two measurement locations. The ASFM measurement plane, 90 cm downstream of the current meter plane was 20 cm upstream of the edge of the gate slot. There is therefore space for flow to bypass the ASFM section via the gate slot, which is not possible at the current meter plane. Using the uppermost measured ASFM velocity to estimate the vertical component of the velocity in the gap shows that the escapement could be as much as 0.5% of the total flow. The structural members on the frame (the bracing cables, current meter support rods and the vertical plate) may also have contributed to the difference in the flow through their presence upstream of the ASFM transducers. The projected area of the vertical plate is sufficient to produce a wake whose width would be about 1% of the tunnel width.

The random differences between the current meter and ASFM discharges are a combination of the random errors in the two methods. Comparison of both the current meter and ASFM discharges with the relative flows obtained from the Winter-Kennedy taps shows that of the 1.5% random difference, approximately 0.5% is due to the current meters and 1% arises from the ASFM. The unfavourable operating conditions experienced by the ASFM are likely to account for the increased variability in its discharge values. The greater distance over which the ASFM's horizontal component of velocity had to be extrapolated to the lower boundary (because of the constraints on the transducer locations) may also have contributed to the variability in the discharge. Comparisons with current meters under conditions of higher turbulence and no interference have shown closer agreement and less scatter (Lemon et al, 1998).

The mean flow angle profile derived for aligning the current meters may also be compared with the inclination angles computed from the ASFM. The angle profile used for the current meters is a curve fitted to the angle of maximum response of the current meters at 1 metre increments of elevation, averaged over all the angle calculation runs. An average inclination as a function of height was computed for the ASFM data by averaging the flow angles in 1-metre classes for all the runs listed in Table 3. Both profiles are shown in Figure 9.

The ASFM data show more variability with height and are shallower by approximately 3° over the upper two thirds of the intake. The effect of the structural members upstream of the ASFM transducers is a likely cause for the difference.

## **Conclusions**

Despite less than ideal operating conditions for the ASFM, good agreement was obtained between the discharges measured by the two methods over a range of flows. A systematic difference of 1.6% observed between the results of the two methods may be the result of an unavoidable separation between the two measurement planes and the presence upstream of the current meters and their supporting structures. Higher variability in the ASFM discharges (approximately twice that of the current meters) is due to the relatively low turbulence level in the flow caused by the removal of the trash rack and interference from the current meters and supporting structures mounted upstream of the ASFM. Under proper operating conditions, the ASFM is capable of the accuracy required to measure turbine discharge in the field.

## **Acknowledgements**

Partial funding for ASL Environmental Sciences Inc.'s participation in the tests was provided by the National Research Council of Canada's IRAP program. The ASL authors wish to thank Hydro-Québec for its support and assistance in providing access to the Laforge-2 site, and logistical support for the ASL field crew. The ASFM hardware and software were built by M. Clarke and R. Chave, respectively, of ASL Environmental Sciences.

## **References**

Birch, R. and D. Lemon, 1993. Acoustic flow measurements at the Rocky Reach Dam. Proc. WaterPower '93, ASCE, 2187-2196.

Clifford, S.F. and D.M. Farmer, 1983. Ocean flow measurements using acoustic scintillation. J. Acoust. Soc. Amer., 74 (6). 1826-1832.

Farmer, D.M. and S.F. Clifford, 1986. Space-time acoustic scintillation analysis: a new technique for probing ocean flows. IEEE J. Ocean. Eng. OE-11 (1), 42 - 50.

Farmer, D.M., S.F. Clifford and J.A. Verrall, 1987. Scintillation structure of a turbulent tidal flow. J. Geophys. Res. 92 (C5), 5369 - 5382.

Ishimaru, A., 1978. Wave Propagation and Scattering in Random Media. Academic Press, N.Y. 572 pp.

Lawrence, R.S., G.R. Ochs and S.F. Clifford, 1972. Use of scintillations to measure average wind across a light beam. Appl. Opt., Vol. 11, pp. 239 - 243.

Lemon, D. D., C. W. Almquist, W. W. Cartier, P.A. March and T. A. Brice 1998. Comparison of turbine discharge measured by current meters and Acoustic Scintillation Flow Meter at Fort Patrick Henry power plant. Proc. HydroVision 98, Reno, 1998.

Lemon, D.D. and D.M. Farmer, 1990. Experience with a multi-depth scintillation flowmeter in the Fraser estuary. Proc. IEEE Fourth Working Conference on Current Measurement, Clinton, MD. April 3-5, 1990. 290 - 298.

Lemon, D. D. 1993. Flow measurements by acoustic scintillation drift in the Fraser River estuary. Proc. IEEE Oceans '93, II-398 to II-403.

Lemon, D. D. 1995. Measuring intake flows in hydroelectric plants with an acoustic scintillation flowmeter. Waterpower '95, ASCE, 2039 - 2048.

Lemon, D. D. and P. W. W. Bell 1996. Measuring hydraulic turbine discharge with the Acoustic Scintillation Flow Meter. Proc. IGHEM, Montreal, 1996.

Proulx, G. and N. Caron 1998. Effect of the trash racks on the discharge measurement in a low head power plant. Proc. IGHEM, Reno, 1998.

Proulx, G. and J.-M. Lévesque 1996. Flow angle measurement with current meters at the La Grande-1 power plant. Proc. IGHEM, Montreal, 1996.

Wang T.I., G.R. Ochs and R.S. Lawrence, 1981. Wind measurements by the temporal cross-correlation of the optical scintillations. Appl. Opt., Vol. 20, pp. 4073 - 4081.